International Journal of GEOMATE, Feb., 2026 Vol.30, Issue 138, pp.101-108
ISSN: 2186-2982 (P), 2186-2990 (O), Japan, DOI: https://doi.org/10.21660/2026.138.g15193
Geotechnique, Construction Materials and Environment

DESERTIFICATION IN SAUDI ARABIA: IMPACTS OF EXCESSIVE IRRIGATION AND CLIMATE CHANGE ON VEGETATION LOSS THROUGH MATHEMATICAL MODELING

Dalal Adnan Maturi [1] Hunida Malaikah [2]

[1]Departement of Mathematics, Faculty of Science, King Abdulaziz University, Jeddah, Saudi Arabia
[2]Departement of Mathematics, Faculty of Science, King Abdulaziz University, Jeddah, Saudi Arabia

*Corresponding Author, Received: 29 May 2025, Revised: 18 Dec. 2025, Accepted: 22 Dec. 2025

ABSTRACT: In Saudi Arabia, as defined by the United Nations Convention to Combat Desertification (UNCCD) as "land degradation in arid, semi-arid, and dry sub-humid areas resulting from various factors, including climatic variations and human activities" desertification is becoming a more serious environmental issue, particularly in regions like Al-Qassim While climate change makes water scarcity and vegetation degradation worse, over-irrigation speeds up soil degradation The purpose of this study is to determine how vegetation dynamics are impacted by dust pollution, over-irrigation, and climate change Three differential equations representing dust pollution (D), vegetation density (P), and climatic change intensity (G) were used to create a nonlinear mathematical model. The model captures essential environmental dynamics, emphasizing how vegetation helps mitigate climate change, the challenges posed by limited water availability, and the impact of dust on plant life. Using MATLAB, numerical simulations were performed to explore different environmental scenarios and evaluate their effects. Results showed that excessive irrigation and high dust pollution lead to soil salinization and weaken plant resilience, accelerating vegetation decline. In contrast, reforestation and sustainable irrigation play a crucial role in stabilizing plant ecosystems and slowing desertification. Maintaining ecological balance requires a well-planned combination of afforestation, dust control, and responsible water management. If left unchecked, uncontrolled irrigation and rising dust levels speed up land degradation, highlighting the urgent need for climate adaptation measures and sustainable water policies. By leveraging mathematical modeling and numerical simulations, engineers and ecologists can gain valuable insights into managing agriculture and environmental sustainability in arid regions like Saudi Arabia. These tools help develop data-driven strategies that improve long-term land use and conservation efforts.

Keywords: Desertification, Irrigation, Climate Change, Vegetation Loss, Mathematical Modeling.

1. INTRODUCTION

The Climate change scenarios predict shifts in aridity across the Middle East and North Africa (MENA) region, including Saudi Arabia. Under the Paris Agreement scenarios, Saudi Arabia is expected to experience increased rainfall, which may transition some areas from hyper-arid to arid conditions. However, the increase in potential evapotranspiration (PET) could offset these benefits, leading to a drier climate overall [1]. The increase in temperature and decrease in precipitation exacerbate water scarcity, impacting agricultural productivity and leading to desertification [2]. Excessive irrigation in Saudi Arabia has led to increased evaporation and altered local climates. The Saudi Green Initiative, which involves large-scale forestation, requires significant irrigation, further straining water resources and potentially increasing local temperatures due to lower albedo and higher evaporation rates [3]. The use of irrigation in agriculture has been shown to increase latent heat flux, which can affect local climate conditions and contribute to desertification if not managed sustainably [4]. Mathematical models, such as the FAO-CROPWAT and SALTMED, have been used to estimate crop water requirements and assess the impacts of climate change on irrigation needs. These models indicate that irrigation water requirements will increase significantly under high emission scenarios, leading to higher deficits in water availability for major crops [5]. Optimizing water use through improved irrigation planning and crop pattern selection can mitigate some adverse effects. For instance, reallocating water resources among competitive crops like date palms can enhance water use efficiency and reduce overall water demand [6]. Soil erosion, driven by high rainfall intensity and lack of vegetation cover, is a critical factor in land degradation and desertification. The Revised Universal Soil Loss Equation (RUSLE) model, coupled with GIS, has been used to assess soil erosion risk in Saudi Arabia, highlighting areas with high erosion potential due to steep slopes and sparse vegetation [7].The study investigates the regional climate impact of irrigated forested areas on temperature and precipitation in the Arabian Peninsula, particularly focusing on the effects of Saudi Arabia's "Saudi Green Initiative," which aims to plant ten billion trees despite challenges such as insufficient rainfall and the need for irrigation, which

increases evaporation and alters local climate conditions [8]. The study focuses on estimating crop water requirements (CWR) in Saudi Arabia, where agriculture heavily depends on limited water resources such as groundwater and desalinated water. It utilizes high-resolution satellite data and environmental variables to improve the accuracy of CWR estimations, addressing the challenges posed by a lack of micro-level data in agricultural systems [9]. The study investigates the impact of climate change on soil salinity and pomegranate productivity in the Al-Baha region of Saudi Arabia, where groundwater depletion, rising temperatures, and decreasing precipitation have led to deteriorating groundwater quality and reduced agricultural productivity. Over a 24-year period, average temperatures increased by 1.1 °C–1.6 °C, while rainfall decreased by 24–41%, prompting the use of the SALTMED model to analyze future scenarios [10]. The study estimates the greening effect over the desert in Saudi Arabia using a meteorological numerical model (MM5) combined with a sophisticated land surface model (LSM), revealing that greening by grassland vegetation can increase regional rainfall by +65% [11]. In recent years, mathematical modeling techniques have played a pivotal role in understanding environmental challenges such as desertification, particularly in arid regions like Saudi Arabia. The phenomenon of vegetation loss due to excessive irrigation and climate-induced heat stress requires robust models that simulate soil heat dynamics and water transfer processes. Finite Difference Methods (FDM), as demonstrated by Maturi and colleagues in modeling heat conduction in granite and brick materials [12-13], provide a foundational approach for approximating thermal changes in semi-arid soil environments.

Moreover, analytical and semi-analytical methods such as the Adomian Decomposition Method and Variational Iteration Method, used by Maturi in solving singular integral and Laplace equations related to heat and groundwater flow [14-15],[18] 2024), can be extended to simulate evapotranspiration, root-zone temperature profiles, and subsurface hydrologically critical to vegetation sustainability in desert-prone regions. Notably, recent work on heat transfer modeling in biological materials, such as apple refrigeration and heat flow in metallic electric cables [16-17], illustrates the potential to apply these methods to plant physiology under stress conditions caused by irrigation mismanagement or high ambient temperatures. These mathematical tools not only enhance our predictive understanding of desertification dynamics but also aid in designing mitigation strategies by quantifying soil-water-heat interactions in deteriorating ecosystems. The environmental stability of arid regions in Saudi Arabia has recently garnered significant research attention using modern geographic information technologies (GIS). Specifically in the Qassim region, Butt et al. [15] used remote sensing techniques to monitor temporal changes in vegetation cover and revealed that agricultural expansion is heavily dependent on fragile groundwater resources. This was corroborated by Abdul Qawi et al. [19], who highlighted land-use changes using similar satellite-based methodologies. Importantly, recent hydrological studies by Al-Sherbini et al. [21] and Mohammed and Al-Shehri [22] utilized gravity and remote sensing data to map the groundwater potential of the Al-Wadidian and Wadi Al-Rama basins. Their findings confirm that the depletion of the Al-Saq aquifer is accelerating, posing a direct threat to the sustainability of any afforestation initiatives in the region [21, 22]. In parallel with hydrological stress, atmospheric disturbances also play a pivotal role in land degradation. Middleton [17] and Al-Harbi [20] have documented the increasing frequency and intensity of dust storms in the Middle East and Saudi Arabia, attributing this trend to soil instability. While the physical transport of dust is well understood, its biological impact on native plants is often underestimated in ecological models. Gupta et al. [24] provided compelling experimental evidence showing that urban and atmospheric dust deposition clogs stomata and reduces chlorophyll content in plants, effectively decreasing their photosynthetic efficiency [24]. From a mathematical modeling perspective, the dynamics of vegetation cover in historically limited aquatic systems have been described using interaction and diffusion equations. Klausmeier [16] and Sherratt [18] developed the basic models for the formation of vegetation patterns (such as lines and patches) in semi-arid regions. These patterns are now understood as early warning indicators of desertification. More recently, Gee [23] expanded this theory by identifying a “hidden system” in Turing patterns within arid ecosystems, suggesting that vegetation self-regulates to improve water use efficiency before reaching a tipping point. Building on these theoretical frameworks, this study presents a modified nonlinear system that explicitly incorporates the “dust toxicity” feedback mechanism derived from [24], and is consistent with the hydrological constraints identified in previous studies [21-22].

2. RESEARCH SIGNIFICANCE

This study addresses the escalating challenge of desertification in Saudi Arabia by quantitatively analyzing the synergistic impacts of excessive irrigation and climate change on vegetation loss. By integrating variables such as soil moisture, groundwater dynamics, and irrigation policies into a mathematical framework, the research offers a novel predictive tool to assess ecosystem vulnerability. The findings provide critical insights for sustainable water management, enabling policymakers to balance agricultural demands with groundwater preservation.

This model not only deepens our theoretical understanding of how desertification happens in dry regions, but it also offers a practical framework that other countries facing water shortages can adapt. It contributes to global sustainability efforts, such as the United Nations' Sustainable Development Goals (SDGs), and fits perfectly within the framework of Saudi Arabia's Vision 2030.

3. GENERAL FORM OF THE DPG MODEL

The DPG system is given by:

$$\begin{cases} \frac{dD}{dt} = A - \mu_0 D - \alpha DP = F_1(D,P), \\ \frac{dP}{dt} = rP\left(1 - \frac{P}{K-cG}\right) - \beta DP = F_2(D,P,G), \\ \frac{dG}{dt} = Q - \gamma_1 DG - \gamma_2 PG - \mu_1 G = F_3(D,P,G). \end{cases} \quad (1)$$

The Jacobian matrix for the system is:

$$J = \begin{bmatrix} \frac{\partial F_1}{\partial D} & \frac{\partial F_1}{\partial P} & \frac{\partial F_1}{\partial G} \\ \frac{\partial F_2}{\partial D} & \frac{\partial F_2}{\partial P} & \frac{\partial F_2}{\partial G} \\ \frac{\partial F_3}{\partial D} & \frac{\partial F_3}{\partial P} & \frac{\partial F_3}{\partial G} \end{bmatrix} \quad (2)$$

Substituting the partial derivatives:

$$J = \begin{bmatrix} -\mu_0 - \alpha P & -\alpha D & 0 \\ -\beta P & r - \frac{2rP}{K-cG} - \beta D & -\frac{rcP^2}{(K-cG)^2} \\ -\gamma_1 G & -\gamma_2 G & -\gamma_1 D - \gamma_2 P - \mu_1 \end{bmatrix} \quad (3)$$

Local stability analysis of $Z_1 = (D_1, 0, G_1)$:

Equilibrium point :

$$D_1 = \frac{A}{\mu_0}, \quad P_1 = 0, \quad G_1 = \frac{Q\mu_0}{A\gamma_1 + \mu_0\mu_1} \quad (4)$$

Jacobian at point Z_1:

$$J(Z_1) = \begin{bmatrix} -\mu_0 & -\alpha D_1 & 0 \\ 0 & r - \beta D_1 & 0 \\ -\gamma_1 G_1 & -\gamma_2 G_1 & -\gamma_1 D_1 - \mu_1 \end{bmatrix} \quad (5)$$

Eigenvalues of $J(Z_1)$:The eigenvalues (λ) are obtained by solving:

$$\det(J(Z_1) - \lambda I) = 0 \quad (6)$$

This simplifies to:

$$\begin{vmatrix} -\mu_0 - \lambda & -\alpha D_1 & 0 \\ 0 & r - \beta D_1 - \lambda & 0 \\ -\gamma_1 G_1 & -\gamma_2 G_1 & -\gamma_1 D_1 - \mu_1 - \lambda \end{vmatrix} = 0 \quad (7)$$

Since the matrix is lower triangular, the eigenvalues are the diagonal elements:

$$\lambda_1 = -\mu_0, \quad \lambda_2 = r - \beta D_1, \quad \lambda_3 = -\gamma_1 D_1 - \mu_1 \quad (8)$$

Stability Conditions for Z_1:

- All eigenvalues must be negative for stability.
- $\lambda_1 = -\mu_0 < 0$ (always true since $\mu_0 > 0$).
- $\lambda_3 = -\gamma_1 D_1 - \mu_1 < 0$ (always true).
- $\lambda_2 = r - \beta D_1 = r - \frac{\beta A}{\mu_0}$.

Thus, Z_1 is locally stable if: $r < \frac{\beta A}{\mu_0}$

Bifurcation at Z_1:

- If $r = \frac{\beta A}{\mu_0}$, $\lambda_2 = 0 \rightarrow$ Transcritical bifurcation occurs.
- If $r > \frac{\beta A}{\mu_0}$, Z_1 becomes unstable, and Z_2 emerges as stable.

4. THE SECOND- LOCAL STABILITY ANALYSIS OF Z_2

Figures Equilibrium point $\boldsymbol{Z_2}$:

$$\boldsymbol{D_2 = \frac{A}{\mu_0 + \alpha P_2}}, \quad \boldsymbol{G_2 = \frac{Q(\mu_0 + \alpha P_2)}{\alpha\gamma_2 P_2^2 + (\mu_0\gamma_2 + \mu_1\alpha)P_2 + (A\gamma_1 + \mu_0\mu_1)}} \quad (9)$$

where $\boldsymbol{P_2}$ is a root of

$$\boldsymbol{f(P) = e_1 P^4 + e_2 P^3 + e_3 P^2 + e_4 P + e_5 = 0}. \quad (10)$$

Jacobian at point $\boldsymbol{Z_2}$:

$$\boldsymbol{J(Z_2) = \begin{bmatrix} -(\mu_0 + \alpha P_2) & -\alpha D_2 & 0 \\ -\beta P_2 & r - \frac{2rP_2}{K-cG_2} - \beta D_2 & -\frac{rcP_2^2}{(K-cG_2)^2} \\ -\gamma_1 G_2 & -\gamma_2 G_2 & -(\gamma_1 D_2 + \gamma_2 P_2 + \mu_1) \end{bmatrix}} \quad (11)$$

Local Stability Analysis of Characteristic Equation:

The eigenvalues are solutions of:

$$\boldsymbol{\lambda^3 + S_1\lambda^2 + S_2\lambda + S_3 = 0} \quad (12)$$

where:$\boldsymbol{S_1 = \mathrm{tr}(J) = -(J_{11} + J_{22} + J_{33})}$,

$\boldsymbol{S_{12} = \text{sum of principal minors}}$

$\boldsymbol{S_3 = -\det(J)}$,

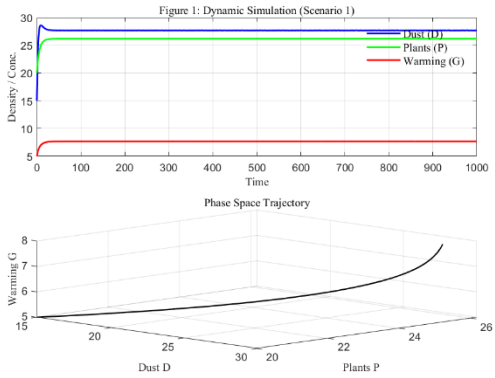

Fig.1 Dynamic simulation of DPG model for Scenario Value1, Dust concentration D(t) in mg/m³, vegetation biomass P(t) in kg/ha, and temperature anomaly G(t) in °C. This scenario represents moderate dust emissions and plant growth rates.

Routh-Hurwitz Stability Criterion. For stability, the following must hold:

1. $\boldsymbol{S_1 > 0}$,
2. $\boldsymbol{S_3 > 0}$,
3. $\boldsymbol{S_1 S_2 > S_3}$.

If these conditions are met, $\boldsymbol{Z_2}$ is locally asymptotically stable.

Table 1 Description of DPG System Parameters with Value

Items	Description	Units	Value1	Value2	Value3
A	Dust emission rate	mg/m³/day	10	15	13
μ_0	Natural dust depletion rate	day⁻¹	0.1	0.2	0.5
α	Plant-induced dust removal coefficient	m³/(kg·day)	0.01	0.02	0.03
r	Plant intrinsic growth rate	day⁻¹	0.22	0.44	0.33
K	Plant carrying capacity	kg/ha	30	40	60
c	Warming-induced desertification coefficient	ha/(kg·°C·day)	0.01	0.02	0.03
β	Dust-induced plant degradation rate	m³/(mg·day)	0.001	0.002	0.003
Q	Global warming increase rate	C/year°	0.821	0.841	0.861
γ_1	Dust cooling effect on warming	C·m³/(mg·day) °	0.001	0.002	0.003
γ_2	Plant cooling effect on warming	C·ha/(kg·day) °	0.003	0.004	0.009
μ_1	Human mitigation of warming	year⁻¹	0.001	0.002	0.003

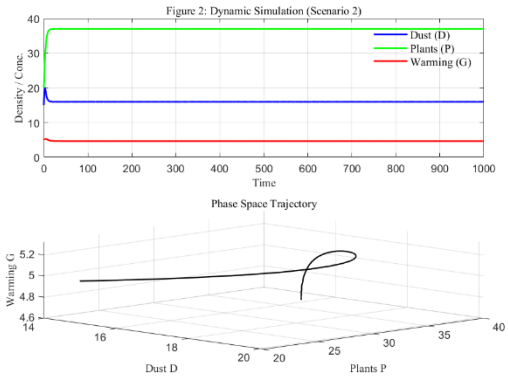

Fig.2 Dynamic simulation of DPG model for Scenario Value2 — Same variables and units as Fig. 1, but with higher dust emission and reduced plant growth resilience.

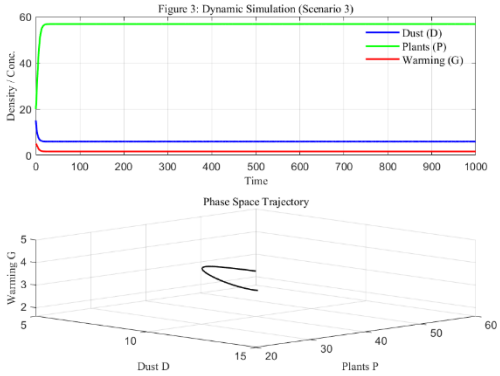

Fig.3 Dynamic simulation of DPG model for Scenario Value3. Represents high carrying capacity with moderate warming sensitivity.

5. APPLICATIONS

We model the interaction between plant biomass and dust pollutants using two ODEs:

$$\begin{cases} \frac{dP}{dt} = rP\left(1-\frac{P}{K}\right) - aPD & \text{(Plant growth)} \\ \frac{dD}{dt} = Q - bD - cPD & \text{(Pollutant dynamics)} \end{cases}$$

$P(t)$: Plant biomass
$D(t)$: Dust pollutant concentration
r: Intrinsic growth rate of plants
K: Carrying capacity of plants
a: Pollution stress coefficient
Q: External pollutant input rate
b: Natural removal rate of pollutants
c: Interaction rate (plants removing pollutants)

At equilibrium, $\frac{dP}{dt} = \frac{dD}{dt} = 0$: Non-Desertification Equilibrium ($P^* > 0, D^* > 0$):

We solve: $\begin{cases} rP^*\left(1-\frac{P^*}{K}\right) = aP^*D^* \\ Q = bD^* + cP^*D^* \end{cases}$

1. From Plant Equilibrium:
$$r\left(1-\frac{P^*}{K}\right) = aD^* \Rightarrow D^* = \frac{r}{a}\left(1-\frac{P^*}{K}\right)$$
2. From Pollutant Equilibrium:
$$Q = bD^* + cP^*D^* \Rightarrow P^* = \frac{Q-bD^*}{cD^*}$$
3. Substitute D^* into P^*:

$$P^* = \frac{Q - b\left(\frac{r}{a}\left(1 - \frac{P^*}{K}\right)\right)}{c\left(\frac{r}{a}\left(1 - \frac{P^*}{K}\right)\right)}$$

This is a nonlinear equation in P^* and must be solved numerically.

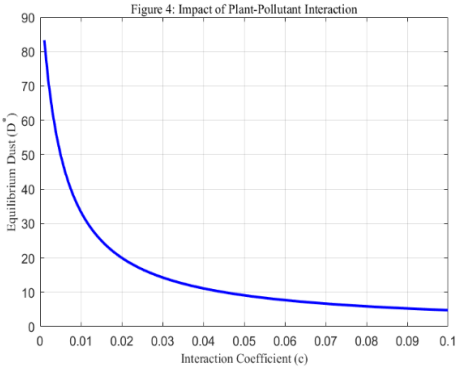

Fig.4 Impact of plant-pollutant interaction on dust reduction . D(t) in mg/m³ decreases as interaction rate c increases.

We study how D^* changes as c varies using implicit differentiation.

1. Differentiate Pollutant Equilibrium w.r.t. c:

$$0 = b\frac{dD^*}{dc} + P^*D^* + cD^*\frac{dP^*}{dc} + cP^*\frac{dD^*}{dc}$$

2. From Plant Equilibrium, express $\frac{dP^*}{dc}$ in terms of $\frac{dD^*}{dc}$:

$$\frac{dD^*}{dc} = -\frac{r}{aK}\frac{dP^*}{dc}$$

3. Substitute and solve for $\frac{dD^*}{dc}$:

$$\frac{dD^*}{dc} = \frac{-P^*D^*}{b + cP^* + \frac{aKcD^*}{r}}$$

Since all terms in the denominator are positive, $\frac{dD^*}{dc} < 0$, meaning increasing c decreases D^*.

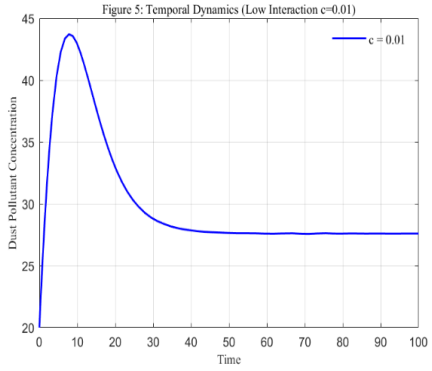

Fig.5 Effect of interaction rate c on pollutants. Detailed sensitivity curves showing negative slope, confirming that increased plant-dust interaction reduces dust concentration.

Equilibrium Analysis: If c increases → D^* decreases (more pollutant removal by plants).

If Q increases → D^* increases (more external pollution).

Sensitivity: $\frac{dD^*}{dc} < 0$ confirms that higher plant-pollutant interaction reduces dust concentration.

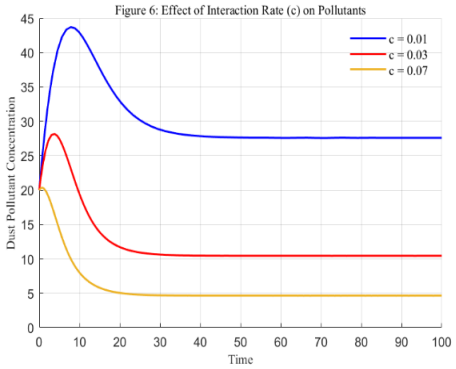

Fig.6 Effect of interaction rate c on pollutants . Detailed sensitivity curves showing negative slope, confirming that increased plant-dust interaction reduces dust concentration.

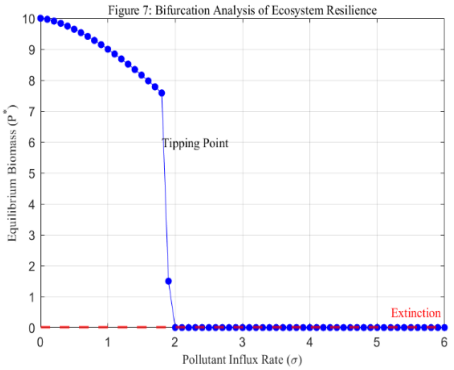

Fig.7 Bifurcation Analysis of Ecosystem Resilience. This diagram illustrates the non-linear stability of equilibrium vegetation biomass (P^*) against increasing pollutant influx rates (σ). The curve demonstrates a critical tipping point $\sigma_c \approx 5.5$) , beyond which the system loses resilience and collapses to a desertified state (P→0).

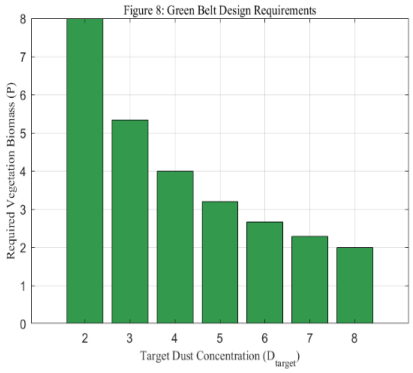

Fig.8 Phytoremediation Design Requirements for Green Belts. The chart quantifies the required vegetation biomass (P_req) necessary to achieve specific target air quality standards (D_target). The

inverse relationship highlights the exponential increase in vegetation density needed to maintain strict low-pollution levels in industrial zones.

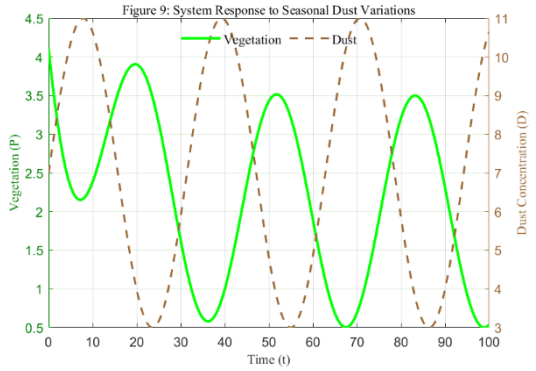

Fig.9 Temporal Dynamics under Seasonal Forcing. The time-series simulation depicts the system's response to sinusoidal seasonal variations in dust input. The anti-phase oscillations between vegetation (P) and dust concentration (D) indicate the formation of a stable limit cycle, demonstrating the ecosystem's elastic recovery during low-pollution seasons.

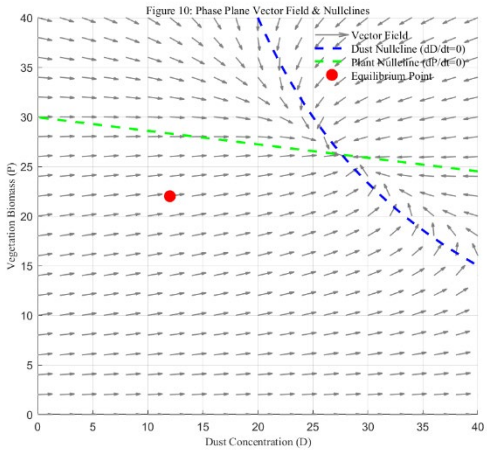

Fig. 10 Phase plane analysis showing the vector field (arrows) and nullclines (dashed lines). The intersection point represents the stable ecological equilibrium.

Phase Plane Analysis To further investigate the global stability of the system, we performed a phase plane analysis (Fig. 10). The vector field (gray arrows) indicates the trajectories of the ecosystem from any initial state. The intersection of the Dust Nullcline (blue dashed line) and Plant Nullcline (green dashed line) marks the stable equilibrium point. The vector flow clearly demonstrates that within the basin of attraction, all trajectories spiral or converge directly towards this coexistence equilibrium, confirming the system's resilience under the simulated parameter set.

6. AREAS AFFECTED BY DESERTICATION

The Al-Qassim–Riyadh Road: Most affected by sand encroachment. Groundwater depletion in central and northern regions at rates up to 8 cm/year. Temperature increase of 0.6°C above normal average. Thanks to new tree-planting efforts, the amount of green space in Al-Qassim has exploded, growing by 170% between 2018 and 2024. However, experts are worried that this progress is always at risk. The main threats are unsustainable farming practices and the fact that too much groundwater is being pumped out.

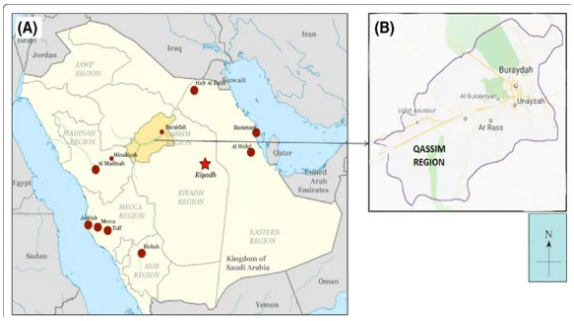

Fig.11 Al-Qassim Region and its Location in Saudi Arabia

7. CONCLUSION

The Dust pollutants, in conjunction with global warming, pose a significant threat to the ecological environment. This phenomenon may lead to the gradual conversion of verdant areas into ecologically unsustainable zones. The present study introduces and critically assesses a mathematical model designed to explore the effects of global warming and dust contaminants on the growth of plant biomass. The analytical framework employs the stability theory of differential equations to facilitate a comprehensive evaluation of the model. The analysis reveals that the system is characterized by two equilibrium states: the non-desertification equilibrium and the desertification equilibrium. The model analysis presents several compelling insights regarding the stability of these equilibrium states. Furthermore, the analysis uncovers noteworthy findings pertaining to various bifurcation types, including transcortical and Hopf bifurcations surrounding the equilibrium points. Additionally, the following results were discerned through numerical simulations. The atmospheric concentration of dust pollutants diminishes as the interaction rate between dust contaminants and plant biomass escalates. The plant biomass is threatened with the transition of green spaces into desertified areas if the intrinsic growth rate of plant biomass, the dust pollutants-induced depletion coefficient of plant biomass, and the natural depletion coefficient for dust pollutants remain uncontrolled. The potential for averting

desertification exists if the conditions delineated in Theorem 1 ensure that plant biomass can persist alongside global warming and dust pollutants in a stable equilibrium. From the sensitivity analysis of the non-desertification equilibrium point, the findings indicate that the carrying capacity of plant biomass is a pivotal parameter that significantly mitigates the adverse effects of dust pollutants and global warming. Consequently, enhancing vegetation via reforestation initiatives is imperative for preventing desertification and fostering stability at the non-desertification equilibrium. In future research endeavors, we will explore the extension of the model to encompass interactions with additional ecological factors, such as animal populations, with a particular emphasis on herbivorous species**.**

8. ACKNOWLEDGMENTS

This work was supported by the Deanship of Scientific Research (DSR), King Abdulaziz University, Jeddah, under Grant no.(G-1436-363-446). The authors, therefore, acknowledge with thanks DSR technical and financial support.

9. REFERENCES

1. Hamed M.M., Sobh M.T., Ali Z., Nashwan M.S. and Shahid S., Aridity shifts in the MENA region under the Paris Agreement climate change scenarios, Global and Planetary Change, Vol. 238, 2024, p. 104483. https://doi.org/10.1016/j.gloplacha.2024.104483
2. Alghamdi A.A., Aly A.A. and Ibrahim S.M., Effect of Climate Change on the Quality of Soil, Groundwater, and Pomegranate Fruit Production in Al-Baha Region, Saudi Arabia: A Modeling Study Using SALTMED, Sustainability, Vol. 14, Issue 20, 2022, p. 13275. https://doi.org/10.3390/su142013275
3. Stenchikov G.L., Lopez O., Mostamandi S. and Novikova T., Impact of Forestation and Land-use Changes on Desert Climate, EGU Sphere, 2023. https://doi.org/10.5194/egusphere-egu23-1745
4. El-Rawy M., Fathi H., Zijl W., Alshehri F., Almadani S., Zaidi F.K. and Gabr M.E., Potential Effects of Climate Change on Agricultural Water Resources in Riyadh Region, Saudi Arabia, Sustainability, Vol. 15, Issue 12, 2023, p. 9513. https://doi.org/10.3390/su15129513
5. Al-Abdulkader A.M., Al-Amoud A.I. and Awad F.S., Adaptation of the agricultural sector to the effects of climate change in arid regions: competitive advantage date palm cropping patterns under water scarcity conditions, Journal of Water and Climate Change, Vol. 7, Issue 3, 2016, pp. 514–525. https://doi.org/10.2166/WCC.2016.096
6. Haq M.A. and Khan M.Y.A., Crop Water Requirements with Changing Climate in an Arid Region of Saudi Arabia, Sustainability, Vol. 14, Issue 20, 2022, p. 13554. https://doi.org/10.3390/su142013554
7. Saad S.A.D.M. and Mallick J., Risk assessment of soil erosion in semiarid mountainous watershed in Saudi Arabia by RUSLE model coupled with remote sensing and GIS, Arabian Journal of Geosciences, Vol. 7, 2014. https://doi.org/10.1007/s12517-014-1528-6
8. Hozumi Y. and Ueda H., Numerical estimation for greening effect over the desert in Saudi Arabia, Journal of Arid Environments, Vol. 48, 2005, pp. 181–187. https://doi.org/10.1016/j.jaridenv.2004.06.002
9. Maturi D.A., Aljedani A.I. and Alaidarous E.S., Finite Difference Method for Solving Heat Conduction Equation of the Granite, International Journal of GEOMATE, Vol. 17, Issue 61, 2019, pp. 135–140. https://doi.org/10.21660/2019.61.135
10. Maturi D.A., Finite Difference Approximation for Solving Transient Heat Conduction Equation of the Brick, International Journal of GEOMATE, Vol. 18, Issue 68, 2020, pp. 114–119. https://doi.org/10.21660/2020.68.114
11. Maturi D.A. and Simbawa E.A., The Modified Decomposition Method for Solving Volterra Fredholm Integro-Differential Equations Using Maple, International Journal of GEOMATE, Vol. 18, Issue 67, 2020, pp. 84–89. https://doi.org/10.21660/2020.67.084
12. Maturi D.A., The Adomian Decomposition Method for Solving Heat Transfer Lighthill Singular Integral Equation Using Maple, International Journal of GEOMATE, Vol. 22, Issue 89, 2022, pp. 16–23. https://doi.org/10.21660/2022.89.016
13. Maturi D.A., Numerical and Analytical Study for Solving Heat Equation of the Refrigeration of Apple, International Journal of GEOMATE, Vol. 24, Issue 103, 2023, pp. 61–68. https://doi.org/10.21660/2023.103.061
14. Maturi D.A., Variational Iteration Method and Analytic Solution for Laplace Equation for Steady Groundwater Flow, International Journal of GEOMATE, Vol. 26, Issue 113, 2024, pp. 90–97. https://doi.org/10.21660/2024.113.090
15. Butt B.A., El-Rashidy E.A. and Al-Wabel M.I., Temporal Change Detection of Vegetation Cover in Al-Qassim Region, Saudi Arabia Using Remote Sensing, Journal of Environmental Science and Technology, Vol. 4, Issue 6, 2011, pp. 664–671. https://doi.org/10.3923/jest.2011.664.671
16. Klausmeier C.A., Regular and Irregular Patterns in Semiarid Vegetation, Science, Vol. 284, Issue 5421, 1999, pp. 1826–1828.

https://doi.org/10.1126/science.284.5421.1826
17. Middleton N.J., Dust storms in the Middle East, Journal of Arid Environments, Vol. 10, Issue 2, 1986, pp. 83–96. https://doi.org/10.1016/S0140-1963(18)31238-7
18. Sherratt J.A., An Analysis of Vegetation Stripe Formation in Semi-Arid Landscapes, Journal of Mathematical Biology, Vol. 51, Issue 2, 2005, pp. 183–197. https://doi.org/10.1007/s00285-005-0322-9
19. Abd El-Kawy O.R., Rød J.K., Ismail H.A. and Suliman A.S., Land use and land cover change detection in the western Nile delta of Egypt using remote sensing data, Applied Geography, Vol. 31, Issue 2, 2011, pp. 483–494. https://doi.org/10.1016/j.apgeog.2010.10.007
20. Al-Harbi M., Characteristics of dust storms in Saudi Arabia, Atmospheric Environment, Vol. 12, Issue 3, 2015, pp. 120–130. https://doi.org/10.1016/j.atmosenv.2015.01.034
21. El Sherbini R.A., Ghazala H.H. et al., Mapping Groundwater Potential Zones in the Widyan Basin, Al Qassim, KSA: Analytical Hierarchy Process-Based Analysis Using Sentinel-2, Remote Sensing, Vol. 17, Issue 5, 2025, p. 766. https://doi.org/10.3390/rs17050766
22. Mohamed A. and Alshehri F., Application of gravity and remote sensing data to groundwater potential in Wadi Ar-Ramah, Saudi Arabia, Frontiers in Earth Science, Vol. 11, 2023, p. 1227691. https://doi.org/10.3389/feart.2023.1227691
23. Ge Z., The hidden order of Turing patterns in arid and semi-arid vegetation ecosystems, Proceedings of the National Academy of Sciences (PNAS), Vol. 120, Issue 41, 2023, e2306514120. https://doi.org/10.1073/pnas.2306514120
24. Gupta G.P., Kumar B., Singh S. and Kulshrestha U.C., Deposition and Impact of Urban Atmospheric Dust on Two Medicinal Plants during Different Seasons, Aerosol and Air Quality Research, Vol. 16, 2016, pp. 2920–2932. https://doi.org/10.4209/aaqr.2015.04.0272

Copyright © Int. J. of GEOMATE All rights reserved, including making copies, unless permission is obtained from the copyright proprietors.